Available online at www.sciencedirect.com
ScienceDirect
Mendeleev Commun., 2014, **24**, 80–81
Mendeleev Communications

Structural characterization of magnetoferritin

Lucia Melníková,*[a] Zuzana Mitróová,[a] Milan Timko,[a] Jozef Kováč,[a] Mikhail V. Avdeev,[b] Viktor I. Petrenko,[b,c] Vasyl M. Garamus,[d] László Almásy[e] and Peter Kopčanský[a]

[a] *Institute of Experimental Physics, Slovak Academy of Sciences, 040 01 Kosice, Slovakia. E-mail: melnikova@saske.sk*
[b] *I. M. Frank Laboratory of Neutron Physics, Joint Institute for Nuclear Research, 141980 Dubna, Moscow Region, Russian Federation*
[c] *Taras Shevchenko National University of Kyiv, 01601 Kyiv, Ukraine*
[d] *Helmholtz-Zentrum Geesthacht, Zentrum für Material- und Küstenforschung, 21502 Geesthacht, Germany*
[e] *Wigner Research Centre for Physics, Institute for Solid State Physics and Optics, H-1525 Budapest, Hungary*

DOI: 10.1016/j.mencom.2014.03.004

The physicochemical characterization of the magnetoferritin biomacromolecule in terms of morphology, structural and magnetic properties shows that iron oxides can be efficiently loaded into apoferritin molecules, preserving their native biocompatible structure and affecting the morphology of the protein shell.

Natural ferritin is the iron-storage protein of animals, plants and bacteria. It is a spherical biomacromolecule with an external diameter of about 12 nm composed of 24 protein subunits arranged as a hollow sphere of approximately 8 nm in diameter. Inside the sphere, iron is stored in the ferric oxidation state as a complex molecule with a crystallographic structure similar to the mineral ferrihydrite.[1] By a suitable chemical process, magnetic iron oxide nanoparticles (Fe_3O_4, γ-Fe_2O_3) can be synthesized in the empty protein shell of ferritin, *i.e*. apoferritin, forming a biocompatible ferrofluid, called magnetoferritin.[2,3] The toxicity and side effects of magnetic nanoparticles in organs and tissues are minimized due to the protein nature of this material, which is important for many applications in cell labeling, biological separation and clinical practice. Their magnetic properties, based on their inducible magnetization, allow them to be heated by externally applied AC magnetic field. It makes them attractive for many applications ranging from various magnetic separation techniques and contrast enhancing agents for MRI to magnetic hyperthermia.[4,5] Magnetoferritin is a promising compound, which can be used as a drug carrier; the protein shell is able to bind tumor cells *via* transferin receptor 1 (TfR1),[6] and the drug can be bound to the protein subunit. In addition to biocompatibility, another advantage for biotechnological applications of magnetoferritin is a relatively short time of controlled synthesis.[7,8]

The main interest of the present study is associated with understanding of certain diseases development mechanism that is in a close relationship with the iron metabolism and iron storage protein, ferritin.[9] In healthy organisms, ferritin is able to store up to 4500 Fe atoms in a ferrihydrite-like mineral core.[10] Many researchers confirmed the presence of magnetite nanoparticles inside pathological tissues,[11,12] which is related to the accumulation of Fe^{2+} ions and defects in the normal storage function of ferritin.[13] This indicates the transformation of ferrihydrite into magnetite and the formation of biogenic magnetoferritin. The precise mode of such a transformation regulated by the biochemistry of organisms (the presence of specific enzymes, biocomplexes, *etc*.) has not been determined. Therefore, in this work, magnetoferritin prepared by *in vitro* chemical synthesis was used as a model system of pathological ferritin. Structural studies of ferritin and magnetoferritin would be useful to elucidate the structural changes of ferritin shell disruption or aggregation, which is observed in the development of cancer or neurodegenerative diseases.[14,15]

In this study, magnetoferritin prepared by controlled chemical synthesis in accordance with a procedure described previously[16] was the test material characterized by dynamic light scattering (DLS), transmission electron microscopy (TEM), small-angle neutron and X-ray scattering (SANS, SAXS) and SQUID magnetometry.

The ζ-potentials of the test apoferritin and magnetoferritin at comparable concentrations of 2.11 and 2.36 mg ml^{-1} were –25.5 and –21.9 mV, respectively. The results confirm the negative charge of the molecule and its good stability. The hydrodynamic molecular diameter of magnetoferritin was measured and compared with that of apoferritin by a dynamic light scattering technique at a protein concentration of 0.3 g dm^{-3} in both solutions (Figure 1).

Generally, the hydrodynamic diameter is larger than the theoretical size because it indicates the effective size of the hydrated/solvated molecule. In comparison with apoferritin hollow sphere (D_{hydr} = 14.14 nm), the hydrodynamic diameter of magnetoferritin increases (D_{hydr} = 19.54 nm). This increase can be related to a deformation of the particles upon loading with iron oxide and to the presence of a fraction of aggregated particles.

Transmission electron microscopy showed the presence of well-defined rounded nanocrystallites (Figure 2) with an average diameter of 5 nm.

The electron diffraction of magnetoferritin samples confirmed the face-centered cubic crystalline structure of the ferrous phase, but it is impossible to distinguish between magnetite (Fe_3O_4) and maghemite (γ-Fe_2O_3). More information can be obtained by magneto-optical birefringence or Faraday rotation studies.[17,18]

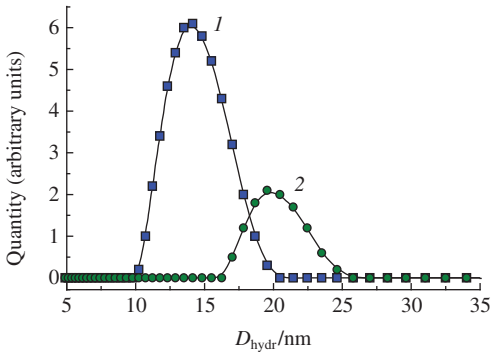

Figure 1 Size distributions of (*1*) apoferritin and (*2*) magnetoferritin as revealed by DLS.

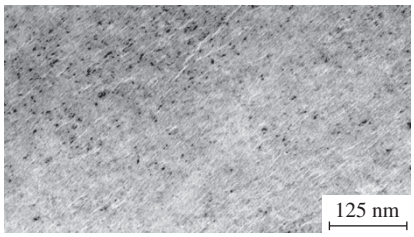

Figure 2 TEM image of magnetoferritin.

Small-angle neutron scattering measurements were performed on a Yellow Submarine instrument operating at the Budapest Neutron Centre.[19] Samples were prepared by redispersing apoferritin and magnetoferritin in D_2O from dry powder to form a 2 wt% solution.

Figure 3 compares the scattering data from pure (unloaded) apoferritin with the scattering of magnetoferritin. For both solutions, the minima and maxima characteristic of the spherical shell form factor of apoferritin are seen. For magnetoferritin, the oscillations are less pronounced, indicating that the spherical form of the protein is only partly preserved. The relative weakening of the characteristic shell structure is attributed to a deformation of the protein shell upon loading, leading to a decrease in the spherical symmetry of the molecules. The increase in the scattering intensity at small values of q shows that a fraction of the molecules aggregates to loose objects of sizes larger than 200 nm. The experimental data were modeled using the hollow spherical shell model of apoferritin and aggregated spherical shell particles for magnetoferritin. The solution contains both aggregated and unaggregated particles, and the used modeling could not distinguish these populations; therefore, the fraction of aggregated particles could not be extracted from the data. Small-angle X-ray scattering data confirmed that the aggregates contain iron oxide.

The magnetic properties of magnetoferritin were studied using a SQUID magnetometer in magnetic fields up to 4000 kA m^{-1}. The samples show superparamagnetic behaviour without hysteresis at room temperature (Figure 4). Using the particle sizes obtained by TEM and assuming magnetite, the saturation magnetization of 8 A m^2 kg^{-1} was calculated. The observed magnetization is lower

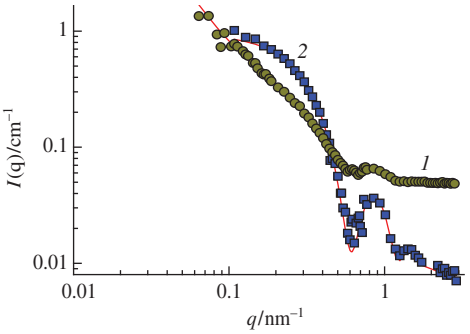

Figure 3 SANS data for (*1*) magnetoferritin and (*2*) apoferritin dispersions in D_2O. The solid lines are model fits of a spherical shell to the apoferritin data and the same model including aggregated particles for the magnetoferritin data.

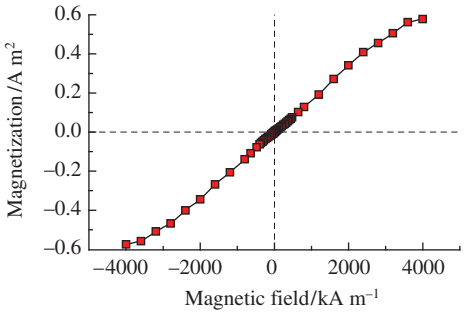

Figure 4 Field dependence of magnetoferritin magnetization at 280 K.

by an order of magnitude than this value, indicating that the magnetic core of magnetoferritin presumably consists of mixed hematite and magnetite. The magnetization curves measured at 2 K below a blocking temperature (T_b = 26 K) showed the hysteresis with a coercive field of 20 kA m^{-1}. The magnetization measured at 5 K undergoes a slow approach to saturation at a field that we can achieve.

In conclusion, the synthesized materials demonstrate a superparamagnetic behaviour; the structure determined by TEM and scattering shows that magnetic nanoparticles are confined in the spherical protein shell with particle diameters of about 5 nm, thus, not filling the entire available space. The protein structure slightly changes upon loading, and this change can be attributed to the effect of iron oxides binding and ordering inside the protein cavity of magnetoferritin. Further experiments, for example, contrast variation SANS methods, would give more detailed information concerning the protein and the magnetic structure of magnetoferritin with different loading factors, to reveal how the iron oxides affect protein conformation. Clarification of these effects could have a major impact in biomedicine for understanding the role of magnetite in connection with aggregation processes in the development of neurodegenerative diseases.

This work was supported by the Structural Funds of European Union, Centre of Excellence of SAS Nanofluid and VEGA 0041, 0045 (project nos. 26220120021, 26220220005 and 26110230061) and the Slovak Research and Development Agency (contract no. APVV 0171-10). The neutron scattering experiments were supported by the European Commission under the 7th Framework Program through the Key Action: Strengthening the European Research Area, Research Infrastructures (Grant Agreement no. 283883 NMI3). L. A. acknowledges the support of the Hungarian Scholarship Board for a short research stay at the IEP SAS.

References

1 N. D. Chasteen and P. M. Harrison, *J. Struct. Biol*., 1999, **126**, 182.
2 F. C. Meldrum, B. R. Heywood and S. Mann, *Science*, 1992, **257**, 522.
3 J. W. Bulte, T. Douglas, S. Mann, R. B. Frankel, B. M. Moskowitz, R. A. Brooks, C. D. Baumgarner, J. J. Vymazal and A. Frank, *Invest. Radiol*., 1994, **29**, 214.
4 S. Mann and F. C. Meldrum, *Adv. Mater.*, 1991, **3**, 316.
5 D. P. E. Dickson, *J. Magn. Magn. Mater*., 1999, **203**, 46.
6 K. Fan, C. Cao, Y. Pan, D. Lu, D. Yang, J. Feng, L. Song, M. Liang and X. Yan, *Nat. Nanotechnol*., 2012, **7**, 459.
7 K. K. W. Wong, T. Douglas, S. Gider, D. D. Awschalom and S. Mann, *Chem. Mater.*, 1998, **10**, 279.
8 M. J. Martínez-Pérez, R. de Miguel, C. Carbonera, M. Martínez-Júlvez, A. Lostao, C. Piquer, C. Gómez-Moreno, J. Bartolomé and F. Luis, *Nanotechnology*, 2010, **21**, 465707.
9 J. F. Collingwood, R. K. K. Chong, T. Kasama, L. Cervera-Gontard, R. E. Dunin-Borkowski, G. Perry, M. Pósfai, S. L. Siedlak, E. T. Simpson, M. A. Smith and J. Dobson, *J. Alzheimers Dis*., 2008, **14**, 235.
10 P. M. Harrison and P. Arosio, *Biochim. Biophys. Acta*, 1996, **1275**, 161.
11 J. L. Kirschvink, A. Kobayashi-Kirschvink and B. J. Woodford, *Proc. Natl. Acad. Sci. USA*, 1992, **89**, 7683.
12 C. Quintana, *Mini-Rev. Med. Chem*., 2007, **7**, 961.
13 F. M. Torti and S. V. Torti, *Blood*, 2002, **99**, 3505.
14 A. A. Alkhateeb and J. R. Connor, *Biochim. Biophys. Acta*, 2013, **1836**, 245.
15 F. Carmona, Ò. Palacios, N. Gálvez, R. Cuesta, S. Atrian, M. Capdevila and J. D. Domínguez-Vera, *Coord. Chem. Rev*., 2013, **257**, 2752.
16 Z. Mitróová, L. Melniková, J. Kováč, M. Timko and P. Kopčanský, *Acta Phys. Pol. A*, 2012, **121**, 1318.
17 M. Koralewski, J. W. Kłos, M. Baranowski, Z. Mitroova, P. Kopčansky, L. Melnikova, M. Okuda and W. Schwarzacher, *Nanotechnology*, 2012, **23**, 355704.
18 M. Koralewski, M. Pochylski, Z. Mitroova, M. Timko, P. Kopcansky and L. Melnikova, *J. Magn. Magn. Mater*., 2011, **323**, 2413.
19 A. Len, J. Füzi, L. Darnay, P. Harmat, K. Koncz and L. Rosta, *Fizikai Szemle*, 2014, **64**, 9.

Received: 29th August 2013; Com. 13/4192